Inorg. Chem. **2007**, *46*, 1388–1395

Enhancement of External Spin–Orbit Coupling Effects Caused by Metal–Metal Cooperativity

Charlotte N. Burress,[†] Martha I. Bodine,[†] Oussama Elbjeirami,[‡] Joseph H. Reibenspies,[†] Mohammad A. Omary,*[,‡] and François P. Gabbaï*[,†]

Department of Chemistry, Texas A&M University, 3255 TAMU, College Station, Texas 77843-3255, and Department of Chemistry, University of North Texas, PO Box 305070, Denton, Texas 76203-5070

Received October 18, 2006

As part of our efforts to discover simple routes to room-temperature phosphors, we have investigated the interaction of bis(pentafluorophenyl)mercury (**1**) or trimeric perfluoro-*o*-phenylene mercury (**2**) with selected arenes (naphthalene, biphenyl, and fluorene). Solution studies indicate that **2**, unlike **1**, quenches the fluorescence of naphthalene. When compared to **1**, the high quenching efficiency of **2** may be correlated to the higher affinity that **2** displays for arenes as well as to more acute external heavy-atom effects caused by the three mercury atoms. In the crystal, the adducts [**1**·naphthalene], [**1**·biphenyl], [**1**·fluorene], and [**2**·fluorene] form supramolecular binary stacks in which the arene approaches the mercury centers of **1** or **2** to form Hg–C π-interactions. Analysis of the electrostatic potential surfaces of the individual components supports the involvement of electrostatic interactions. The luminescence spectra of the adducts show complete quenching of the fluorescence and display heavy-atom-induced emission whose energies and vibronic progressions correspond to the phosphorescence of the respective pure arene. The phosphorescence lifetimes are shortened by 3 or 4 orders of magnitude when compared with those of the free arenes. Taken collectively, the structural, photophysical, and computational results herein suggest that the proximity of the three mercury centers serves to enhance the Lewis acidity of **2**, which becomes a better acceptor and a more effective heavy-atom effect inducer than **1**.

Introduction

Organomercurials featuring electron-withdrawing substituents form adducts with a number of neutral and anionic Lewis basic substrates. For instance, bis(pentafluorophenyl)-mercury (**1**, Chart 1) complexes bromide and iodide to afford T-shaped anionic complexes in which the anion is terminally ligated to the mercury center.[1] In an analogous fashion, trimeric perfluoro-*o*-phenylene mercury (**2**, $[o\text{-}C_6F_4Hg]_3$, Chart 1) complexes halides including bromide and iodide.[2] In both cases, structural studies indicate the occurrence of cooperative effects between the mercury atoms of **2** which simultaneously participate in the binding of the anion. Similar cooperative effects have been observed in adducts involving **2** and a number of neutral or anionic electron rich substrates.[3,4] As part of our contribution to this general area, we found that **2** interacts with aromatic substrates to form extended binary supramolecules in which **2** and the arene

Chart 1. Structures of the Molecules Considered in These Studies

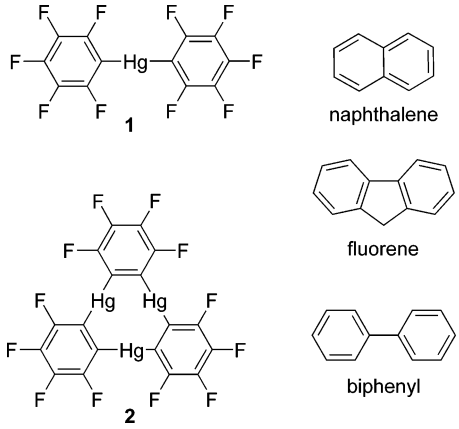

* To whom correspondence should be addressed. E-mail: francois@tamu.edu (F.P.G.), omary@unt.edu (M.A.O.).
[†] Texas A&M University.
[‡] University of North Texas.

(1) Schulz, F.; Pantenburg, I., Naumann, D. Z. *Anorg. Allg. Chem.* **2003**, *629*, 2312.
(2) Shur, V. B.; Tikhonova, I. A.; Yanovsky, A. I.; Struchkov, Y. I.; Petrovskii, P. V.; Panov, S. Y.; Furin, G. G.; Vol'pin, M. Y. *J. Organomet. Chem.* **1991**, *418*, C29−C32.

10.1021/ic061998n CCC: $37.00
Published on Web 01/23/2007

alternate.[5−10] This approach has now been extended to a number of aromatic substrates[11] including pyrene, naphthalene, and biphenyl.[7,8] The mercury centers of the trinuclear complex approach the π-face of the aromatic substrate and engage in polyhapto secondary Hg−C interactions in the 3.3−3.6 Å range. Because of the extended structures of these solids, each arene is surrounded by six mercury atoms. As a result, the arene experiences an intense spin−orbit perturbation[12] manifested by the $T_1 \rightarrow S_0$ monomer phosphorescence of the arene. Moreover, the triplet excited-state lifetimes fall in the millisecond range, which represents a shortening by 3−4 orders of magnitude in comparison to the lifetimes of the free arene.[6] More drastic lifetime shortenings are observed in the case of aromatic N-heterocycles such as *N*-methylcarabazole whose triplet lifetime is reduced by 5 orders of magnitude when complexed to **2**![9] The extent of the external heavy-atom effects induced by **2** is unusually high and exceeds that observed in the presence of internal heavy atoms. For example, the triplet lifetime of naphthalene in [**2**·naphthalene] ($\tau_P = 0.987$ ms)[7] is distinctly shorter than that of the internal heavy-atom containing 1-iodonaphthalene ($\tau_P = 2.50$ ms).[13] To better appreciate the origin of these unusual heavy-atom effects, we have decided to compare the properties of trinuclear **2** to those of its monofunctional analogue, **1**. In this paper, we present a set of structural and solution studies which suggest that cooperative effects are involved in the spin−orbit perturbation that **2** provides to arenes including biphenyl, fluorene, and naphthalene (Chart 1). We also demonstrate that the mononuclear derivative **1** is a useful supramolecular synthon which readily assembles with biphenyl, fluorene, and naphthalene to form room-temperature-phosphorescent supramolecules. These studies are part of our ongoing effort to discover novel materials for organic light emitting diodes.

Experimental Section

General. ***Warning****! Due to the toxicity of the mercury compounds discussed, extra care was taken at all times to avoid contact with solid, solution, and airborne particulate mercury compounds.* The studies herein were carried out in a well-aerated fume hood. Atlantic Microlab, Inc., Norcross, GA, performed the elemental analyses. All commercially available starting materials and solvents were purchased from Aldrich Chemical and VWR, Inc., and used as provided. Compounds **1** and **2** were prepared according to published procedures, and the purity of these starting materials was confirmed by ^{1}H and ^{19}F NMR.[14,15]

Synthesis of Adducts. All compounds were prepared by mixing **1** or **2** with the corresponding arene in CH_2Cl_2 (5−10 mL). Crystals formed upon slow evaporation of the solvent. Reagent quantities, yields, elemental analysis results, and melting points are provided for each adduct hereafter.

[**1**·Naphthalene]: **1** (0.020 g, 0.0374 mmol), naphthalene (0.0048 g, 0.0374 mmol). Yield: 0.0184 g, 92%. Anal. Calcd for $C_{22}H_8F_{10}Hg$: C, 39.86; H, 1.22. Found: C, 39.89; H, 1.05. Mp 184 °C.

[**1**·Biphenyl]: **1** (0.020 g, 0.0374 mmol), biphenyl (0.0058 g, 0.0374 mmol). Yield: 0.0252 g, 98%. Anal. Calcd for $C_{24}H_{10}F_{10}Hg$: C, 41.84; H, 1.46. Found: C, 41.63; H, 1.29. Mp 169 °C.

[**1**·Fluorene]: **1** (0.020 g, 0.0374 mmol), fluorene (0.0062 g, 0.0374 mmol). Yield: 0.0249 g, 95%. Anal. Calcd for $C_{25}H_{10}F_{10}Hg$: C, 42.84; H, 1.44. Found: C, 42.76; H, 1.24. Mp 204 °C.

[**2**·Fluorene]: **2** (0.020 g, 0.0191 mmol), fluorene (0.0030 g, 0.0191 mmol). Yield: 0.022 g, 96%. Anal. Calcd for $C_{31}H_{10}F_{12}Hg_3$: C, 30.71; H, 0.83. Found: C, 30.97; H, 0.76. Mp 312 °C (dec).

Crystal Structure Determinations. X-ray data for [**1**·naphthalene], [**1**·biphenyl], [**1**·fluorene], and [**2**·fluorene] were collected on a Bruker SMART-CCD diffractometer using graphite-monochromated Mo Kα radiation ($\lambda = 0.71073$ Å). Specimens of suitable size and quality were selected and glued onto a glass fiber with freshly prepared epoxy resin. The structure was solved by direct methods, which successfully located most of the non-hydrogen atoms. Subsequent refinement on F^2 using the SHELXTL/PC package (version 6.1) allowed location of the remaining non-hydrogen atoms. Details of the crystal structures can be found in the CIF file.

Theoretical Calculations. The theoretical calculations have been carried out with the Gaussian 98[16] implementations of B3LYP (Becke three-parameter exchange functional (B3)[17] and the Lee−Yang−Parr correlation functional (LYP)[18]) density functional theory (DFT).[19] The DFT calculations used the default SCF convergence for geometry optimizations (10^{-8}). The 6-31G basis sets of Pople and co-workers[20] were used for all the carbon, hydrogen, and fluorine atoms, and the Stuttgart RSC 1997 ECP[21] basis sets were

(3) For a general review, see: Shur, V. B.; Tikhonova, I. A. *Russ. Chem. Bull.* **2003**, *52*, 2539−2554.
(4) Haneline, M. R.; Taylor, R. E.; Gabbaï, F. P. *Chem.—Eur. J.* **2003**, *9*, 5188−5193.
(5) Haneline, M. R.; Gabbaï. F. P. *Angew. Chem., Int. Ed.* **2004**, *43*, 5471−5474.
(6) Haneline, M. R.; Taylor, R.; Gabbaï, F. P. *Chem.—Eur. J.* **2003**, *9*, 5188−5193.
(7) Omary, M.; Kassab, R.; Haneline, M.; Elbjeirami, O.; Gabbaï, F. P. *Inorg. Chem.* **2003**, *42*, 2176−2178.
(8) Haneline, M.; Tsunoda, M.; Gabbaï, F. P. *J. Am. Chem. Soc.* **2002**, *124*, 3737−3742.
(9) Burress, C.; Elbjeirami, O.; Omary, M.; Gabbaï, F. P. *J. Am. Chem. Soc.* **2005**, *127*, 12166−12167.
(10) Taylor, T. J.; Gabbaï, F. P. *Organometallics* **2006**, *25*, 2143−2147.
(11) Tikhonova, I. A.; Tugashov, K. I.; Dolgushin, F. M.; Yakovenko, A. A.; Strunin, A. B.; Petrovskii, P. V.; Furin, G. G.; Shur, V. B. *Inorg. Chim. Acta* **2006**, *359*, 2728−2735.
(12) The spin−orbit coupling constant (ξ) for the 5d orbital is ~5 100 cm^{-1} in species with a 5d^{10} valence configuration: Griffith, J. S. *Theory of Transition Metal Ions*; Cambridge University Press: Cambridge, 1964.
(13) McClure, D. S. *J. Chem. Phys.* **1949**, *17*, 905−913.
(14) Sartori, P.; Golloch, A. *Chem. Ber.* **1968**, *101*, 2004−2009.
(15) Jukes, A. E.; Gilman, H. *J. Organomet. Chem.* **1969**, *17*, 145−148.
(16) Frisch, M. J.; Trucks, G. W.; Schlegel, H. B.; Scuseria, G. E.; Robb, M. A.; Cheeseman, J. R.; Zakrzewski, V. G.; Montgomery, J. A.; Stratmann, R. E.; Burant, J. C.; Dapprich, S.; Millam, J. M.; Daniels, A. D.; Kudin, K. N.; Strain, M. C.; Farkas, O.; Tomasi, J.; Barone, V.; Cossi, M.; Cammi, R.; Mennucci, B.; Pomelli, C.; Adamo, C.; Clifford, S.; Ochterski, J.; Petersson, G. A.; Ayala, P. Y.; Cui, Q.; Morokuma, K.; Malick, D. K.; Rabuck, A. D.; Raghavachari, K.; Foresman, J. B.; Cioslowski, J.; Ortiz, J. V.; Stefanov, B. B.; Liu, G.; Liashenko, A.; Piskorz, P.; Komaromi, I.; Gomperts, R.; Martin, R. L.; Fox, D. J.; Keith, T.; Al-Laham, M. A.; Peng, C. Y.; Nanayakkara, A.; Gonzalez, C.; Challacombe, M.; Gill, P. M. W.; Johnson, B.; Chen, W.; Wong, M. W.; Andres, J. L.; Gonzalez, A. C.; Head-Gordon, M.; Replogle, E. S.; Pople, J. A. *Gaussian 98*, revision A.11.3; Gaussian, Inc.: Pittsburgh, PA, 1998.
(17) Becke, A. D. *J. Chem. Phys.* **1993**, *98*, 5648.
(18) Lee, C.; Yang, W.; Parr, R. G. *Phys. Rev. B: Condens. Matter* **1988**, *37*, 785.
(19) Parr, R. G.; Yang, W. *Density Functional Theory of Atoms and Molecules*; Oxford University Press: New York, 1989.
(20) Ditchfield, R.; Hehre, W. J.; Pople, J. A. *J. Chem. Phys.* **1971**, *54*, 724.
(21) Bergner, A.; Dolg, M.; Kuchle, W.; Stoll, H.; Preuss, H. *Mol. Phys.* **1993**, *80*, 1431−1441.

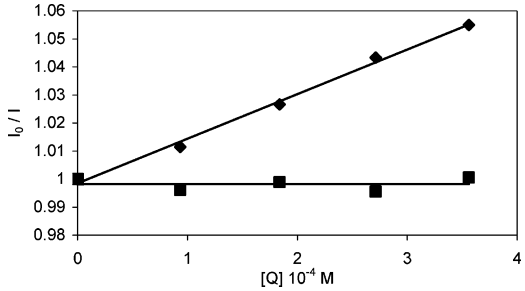

Figure 1. Stern−Volmer plots of the fluorescence quenching of naphthalene (7×10^{-3} M) in CH_2Cl_2 at ambient temperatures with **1** (■; 6×10^{-3} M) and **2** (◆; 5.7×10^{-3} M). The samples were excited at 327 nm, and the emission intensities were monitored at $\lambda_{max} = 337$ nm during the titration.

used for the mercury atom. The structure was constrained to D_{2h} symmetry and then fully optimized, and analytical frequency calculations were performed to ensure that either a minimum or a first-order saddle point was achieved. The electrostatic potential surface calculations were carried out on the optimized structure.

Luminescence Titrations. The solution luminescence spectra were recorded with a SLM/AMINCO, model 8100 spectrofluorometer equipped with a xenon lamp. Titration experiments were performed by adding aliquots of a CH_2Cl_2 solution of **1** (50 μL of 5.7×10^{-3} M) or **2** (50 μL of 6×10^{-3} M) to a quartz cuvette containing 3.00 mL of a 7×10^{-3} M CH_2Cl_2 solution of naphthalene. The samples were excited at 327 nm, and the emission intensities were monitored at 337 nm during the titration. The intensities were corrected for dilution and absorption using the following formula: $I_{corrected} = I_{observed}(V/V_{initial}) \times 10^{(0.5A)}$ (V = volume of solution, $V_{initial}$ = volume of solution before the first addition, A = absorbance at 337 nm).[22]

Photophysical Measurements. Steady-state luminescence spectra were acquired for solution and solid samples with a PTI QuantaMaster model QM-4 scanning spectrofluorometer. The excitation and emission spectra were corrected for the wavelength-dependent lamp intensity and detector response, respectively. Lifetime data were acquired using fluorescence and phosphorescence subsystem add-ons to the PTI instrument. The pulsed excitation source (pulse width = 800−1200 ps) was generated using the 337.1 nm line of the N_2 laser pumping a freshly prepared 5×10^{-3} M solution of the continuum laser dye, Coumarin-540A, in ethanol, the output of which was appropriately tuned and frequency doubled to attain the excitation wavelengths needed based on the luminescence excitation spectra for each compound. Cooling in temperature-dependent measurements was achieved using an Oxford optical cryostat, model Optistat CF, interfaced with a liquid helium tank. All lifetime measurements showed a satisfactory fit to the single-exponential decay function ($R^2 = 0.98-0.99$). Solution studies were carried out on non-deoxygenated samples.

Results and Discussion

Solution Studies. In order to probe for possible cooperative effects in the binding of arenes by the trifunctional Lewis acid **2**, we first studied mixtures of **2** and naphthalene using fluorescence spectroscopy. Incremental addition of **2** to a CH_2Cl_2 solution of naphthalene leads to quenching of the fluorescence (Figure 1). The observed quenching, which results from the spin−orbit perturbation provided by the organomercurial to the arene, indicates that the two molecular components interact in solution. The emission lifetime, which remains constant throughout the titration, points to the preponderance of a static quenching mechanism.[23] In agreement with this view, the Stern−Volmer constant of 159 ± 6 M^{-1} is higher than the value of 97 M^{-1} which can be theoretically predicted from the singlet lifetime of naphthalene and the collisional frequency derived from the Smoluchowski equation.[24] When the same experiment was repeated with **1**, no fluorescence quenching could be observed. The high quenching efficiency of **2** may result from two factors. As a first factor, it can be proposed that **2** possesses an increased affinity for naphthalene possibly originating from the planarity of the molecule, which facilitates the approach and complexation of the aromatic substrate. Although **1** is able to access a planar conformation (vide infra), available crystal structures indicate that the two pentafluorophenyl rings prefer to be twisted,[25] which would hinder the approach and complexation of flat aromatic substrates. As a second factor, we can also invoke the occurrence of more acute external heavy-atom effects in the case of **2** which contains three mercury atoms rather than one. For biphenyl and fluorene, fluorescence quenching experiments could not be carried out because of a large overlap between the absorption spectrum of the quencher **2** and the excitation spectrum of the arene. To further assess the spin−orbit coupling perturbation provided by **1** and **2**, we turned our attention to the study of solid adducts.

Synthesis and Structure of the Adducts. The coordination chemistry of **1** is much less developed than that of **2**. In fact, only a handful of adducts involving **1** have been thus far reported. These adducts involve Lewis basic substrates containing nitrogen,[26] phosphorus, and arsenic[27] as donor atoms. To our knowledge, however, adducts involving unsubstituted arenes have remained unknown. Combination of **1** with naphthalene, biphenyl, or fluorene in CH_2Cl_2 followed by slow evaporation of the solvent leads to the crystallization of [**1**·naphthalene], [**1**·biphenyl], and [**1**·fluorene], whose composition has been confirmed by elemental analysis. These adducts, which are air stable and melt at 184, 169, and 204 °C for [**1**·naphthalene], [**1**·biphenyl], and [**1**·fluorene], respectively, have been studied by single-crystal X-ray analysis. In the solid state, these adducts form extended binary stacks where molecules of **1** alternate with the arene (Figure 2). In all three adducts, there are no unusual intramolecular bond distances and angles in the structure of the individual components. The closest known analogue of such binary compounds is an adduct involving **1** and 2,2′-dipyridyl diselenide.[28] This adduct forms

(22) Lakowicz, J. *Principles of Fluorescence Spectroscopy*; Kluwer/Plenum: New York, 1999.

(23) The lifetime data can be found in the Supporting Information.

(24) The diffusion-controlled rate constant, k_q, can be calculated using Smoluchowski's equation; k_q can then be used to calculate the Stern−Volmer constant (K_{SV}) for a collisional-quenching scenario. More details are available in the Supporting Information. Examples of these types of calculations are found in ref 22, pp 241−242.

(25) Kunchur, N. R.; Mathew, M. *Chem. Commun.* **1966**, 71−73.

(26) Puhl, W. H. Henneike, H.F. *J. Phys. Chem.* **1973**, *77*, 558−562.

(27) Canty, A. J.; Gatehouse, B. M. *J. Chem. Soc., Dalton Trans.* **1972**, 511.

(28) Kientiz, C.; Thone, C.; Jones, P. *Inorg. Chem.* **1996**, *35*, 3990−3997.

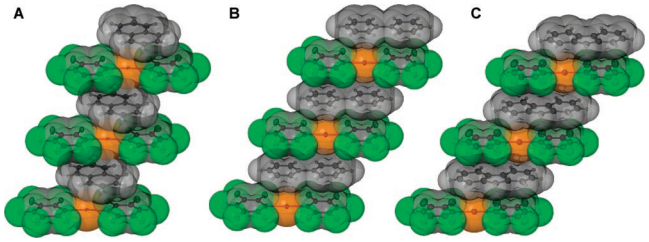

Figure 2. ORTEP view with transparent van der Waals spheres of a stack in each of the structures of [**1**·naphthalene] (A), [**1**·biphenyl] (B), and [**1**·fluorene] (C).

extended stacks that are supported by Hg−Se interactions, rather than Hg−C interactions.

Adduct [**1**·naphthalene] crystallizes in the monoclinic space group $P2_1/c$ with half a molecule of **1** and half a molecule of naphthalene in the asymmetric unit (Table 1, Figure 2A, Figure 3). The naphthalene molecule is weakly π-coordinated to the mercury centers of two neighboring molecules of **1** (Figure 2A). The two mercury centers Hg(1) and Hg(1A) effectively sandwich the naphthalene molecule via η^3-interactions involving the carbon atoms C(7), C(10), and C(11) and their symmetry related equivalents C(7A), C(10A), and C(11A) (Figure 3). These Hg−C interactions fall in the range of 3.21−3.49 Å, which are some of the shortest distances observed in arene adducts of organomercurials[29] and are within the van der Waals radii for Hg (r_{vdw} = 1.73−2.00 Å)[30] and $C_{aromatic}$ (r_{vdw} = 1.7 Å)[31] (Figure 3). As a result of these interactions, the naphthalene molecule is slightly tilted with respect to the plane containing **1** with which it forms an angle of 4.6°. We also note that the naphthalene does not engage in arene−perfluoroarene interactions with the pentafluorophenyl groups of **1**. Adduct [**1**·biphenyl] crystallizes in the triclinic space group *P*-1 with half a molecule of **1** and half a molecule of biphenyl in the asymmetric unit (Table 1 and Figure 4). Unlike in [**1**·naphthalene], one of the pentafluorophenyl groups of the organomercurial forms an arene−perfluoroarene interaction with the biphenyl molecules (Figure 2B). The presence of this interaction is supported by the short distance of 3.65 Å separating the centroids of the phenyl ring containing C(8) and pentafluorophenyl ring containing C(1B) (Figure 4). Cohesion of the components is further assisted by a secondary mercury−π interaction of 3.51 Å involving Hg(1) and C(8) and their symmetry equivalent atoms Hg(1A) and C(8A). As in [**1**·naphthalene], the biphenyl molecule is slightly tilted with respect to the plane containing **1** with which it forms an angle of 4.4°. Both components are planar; the biphenyl occupies a crystallographic inversion center resulting in a Ph−Ph dihedral angle of 0°. This situation differs from that observed in the gas phase where the Ph−Ph dihedral angle is close to 44.4°.[32] According to computations, this twisted conformation corresponds to an energy minimum whereas the flat conformation corresponds to a maximum which is about 2−3 kcal higher in energy.[33] It can be argued that supramolecular Hg−C and arene−perfluoroarene interactions are sufficient to overcome the repulsions present in the flat conformation of biphenyl. The observation of planar biphenyl molecules is a rare phenomenon which has only been reported to occur in a few other supramolecular systems.[34] Adduct [**1**·fluorene] crystallizes in the triclinic space group *P*-1 with half a molecule of **1** and half a molecule of fluorene in the asymmetric unit (Table 1 and Figure 2C). The fluorene molecule, which is affected by positional disorder, was refined as a rigid unit over two positions of equal occupancy. Although the quality of the refinement is satisfactory, a detailed discussion of the intramolecular interaction is somewhat superfluous. It remains that the distance separating the plane of the fluorene molecule to that of **1** is around 3.5 Å, a distance commensurate with the existence of both Hg−C and arene−fluoroarene interactions (Figure 2C).

The structure of **1** was computationally optimized using DFT methods (B3LYP, 6-31G for C and F atoms, and Stuttgart RSC 1997 ECP for the Hg atom). The mercury adopts a linear geometry, and the two pentafluorophenyl rings are twisted by 90.0°, which can be compared to the value of 59.4° determined crystallographically.[25] Since in adducts [**1**·naphthalene], [**1**·biphenyl], and [**1**·fluorene] the molecule of **1** is essentially planar, we repeated the optimization of **1** with its structure constrained to the D_{2h} point group. The resulting calculated geometry corresponds closely to that observed in adducts [**1**·naphthalene], [**1**·biphenyl], and [**1**·fluorene]. These DFT calculations were also used to map the electrostatic potential on the electron density surface of **1** (Figure 5). Examination of the electrostatic potential map shows that the mercury atom and, to some extent, the core of the pentafluorophenyl ring develop a positive character while the fluorine atoms bear most of the negative charges. The electrostatic potential surface of **1** shows an opposite polarization when compared with those of biphenyl, naphthalene, and fluorene, which display a negative potential at their centers and a positive potential at the periphery (Figure 5). The respective positioning of **1** and the arene in the crystal agrees well with the complementarity of the electrostatic potential surfaces of the two components. In turn, the observed structures suggest that electrostatic interactions are partly responsible for the formation of these adducts. Keeping in mind that mercury is soft and polarizable, the involvement of dispersion forces should not be ruled out and may also contribute to the stability of the adducts.

We have previously isolated and characterized complexes [**2**·naphthalene] and [**2**·biphenyl], which can be regarded as the trifunctional analogues of [**1**·naphthalene] and [**1**·biphenyl].[8] To prepare the corresponding trifunctional analogue of [**1**·fluorene], we have synthesized [**2**·fluorene]. Colorless crystals of [**2**·fluorene] can be easily obtained by slow evaporation of a CH_2Cl_2 solution of **2** and fluorene. Elemental analysis confirmed the 1:1 stoichiometry of the

(29) Gardinier, J. R.; Gabbai, F. P. *Dalton Trans.* **2000**, 2861−2865.
(30) Pyykkö, P.; Straka, M. *Phys. Chem. Chem. Phys.* **2000**, *2*, 2489−2493.
(31) Caillet, J.; Claverie, P. *Acta Crystallogr.* **1975**, *A31*, 448−461.
(32) Almenningen, A.; Bastiansen, O.; Fernholt, L.; Cyvin, B. N.; Cyvin, S. J.; Samdal, S. *J. Mol. Struct. (THEOCHEM)* **1985**, *128*, 59.
(33) Grein, Friedrich, *J. Phys. Chem. A* **2002**, *106*, 3823−3827.
(34) (a) Sekiya, R.; Nishikiori, S. *Chem.—Eur. J.* **2002**, *8*, 4803−4810. (b) Biradha, K.; Mahata, G. *Cryst. Growth Des.* **2005**, *5*, 61−63.

Table 1. Crystal Data, Data Collection, and Structure Refinement for [**1**·Naphthalene], [**1**·Biphenyl], [**1**·Fluorene], and [**2**·Fluorene]

	[**1**·naphthalene]	[**1**·biphenyl]	[**1**·fluorene]	[**2**·fluorene]
		crystal data		
formula	$C_{22}H_8F_{10}Hg$	$C_{24}H_{10}F_{10}Hg$	$C_{25}H_{10}F_{10}Hg$	$C_{31}H_{10}F_{12}Hg_3$
fw	662.87	688.91	700.92	2424.32
cryst size (mm)	0.23 × 0.07 × 0.05	0.23 × 0.18 × 0.04	0.45 × 0.11 × 0.03	0.35 × 0.20 × 0.05
crystal syst	monoclinic	triclinic	triclinic	monoclinic
space group	$P2(1)/c$	$P-1$	$P-1$	$P2(1)/c$
a (Å)	9.948(2)	6.3754(13)	7.0988(14)	7.0469(14)
b (Å)	6.8142(14)	8.0460(16)	8.1504(16)	44.805(9)
c (Å)	14.627(3)	10.918(2)	10.740(2)	17.337(4)
α (deg)		90.13(3)	91.37(3)	
β(deg)	105.33(3)	102.04(3)	107.29(3)	91.36(3)
γ (deg)		102.75(3)	108.90(3)	
V (Å^3)	956.3(3)	533.54(19)	556.34(19)	5472.3(19)
Z	2	1	1	4
σ_{calc} (g cm^{-3})	2.302	2.144	2.092	2.943
μ(Mo Kα) (mm^{-1})	8.151	7.309	7.012	16.897
F(000) (e)	620	324	330	4 352
		data collection		
T (K)	110(2)	273(2)	273(2)	110(2)
scan mode	ω	ω	ω	ω
hkl range	$-12 \le h \le 12$ $-8 \le k \le 8$ $-18 \le l \le 18$	$-8 \le h \le 8$ $-10 \le k \le 10$ $-14 \le l \le 14$	$-8 \le h \le 8$ $-9 \le k \le 9$ $-12 \le l \le 14$	$-7 \le h \le 7$ $-49 \le k \le 49$ $-18 \le l \le 19$
measured reflns	7 171	4 739	5 052	34 002
unique reflns [R_{int}]	1873 [0.0272]	2498 [0.0297]	2634 [0.0571]	7851 [0.0305]
reflns used for refinement	1873	2498	2634	7851
absorption correction	SADABS	SADABS	SADABS	SADABS
T_{min}/T_{max}	0.720398	0.660439	0.2275	0.286218
		refinement		
refined parameters	154	165	119	829
R1, wR2 [$I > 2(I)$][a,b]	0.0280, 0.0754	0.0323, 0.0610	0.0457, 0.0991	0.0442, 0.1004
ρ_{fin} (max/min) (e·Å^{-3})	1.913, −0.780	0.541, −0.497	0.615, −0.630	3.546, −1.222

[a] $R1 = (F_o - F_c)/ F_o$. [b] $wR2 = \{[w(F_o^2 - F_c^2)^2]/ [w(F_o^2)^2]\}^{1/2}$; $w = 1/[\sigma^2(F_o^2) + (ap)^2 + bp]$; $p = (F_o^2 + 2F_c^2)/3$; $a = 0.0500$ ([**1**·naphthalene]), 0.050 ([**1**·biphenyl]), 0.012 ([**1**·fluorene]), 0.010 ([**2**·fluorene]); $b = 40.0000$ ([**1**·naphthalene]), 66.0 ([**1**·biphenyl]), 41.0 ([**1**·fluorene]), 141.0 ([**2**·fluorene]).

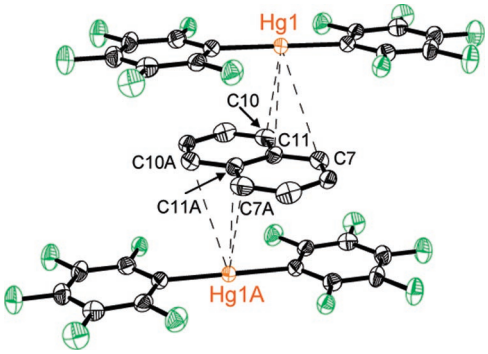

Figure 3. ORTEP view (50% ellipsoid) of a portion of a stack in the structure of [**1**·naphthalene]. Representative intermolecular distances (Å): Hg(1)−C(7) 3.49, Hg(1)−C(10) 3.27, Hg(1)−C(11) 3.21.

adduct. This adduct crystallizes in the monoclinic space group $P2_1/c$ with two independent molecules of [**2**·fluorene] in the asymmetric unit (Table 1). Consequently, there are two crystallographically independent types of stacks which differ by the orientation of the fluorene unit with respect to the trinuclear mercury core of **2** (Figure 6). In both stacks, secondary Hg−π interaction contacts are observed between the aromatic rings of the fluorene molecule and the mercury centers of the trinuclear mercury complex. The resulting Hg−C contacts fall in the range of 3.27−3.39 Å and are thus within the sum of the van der Waals radii of mercury and carbon. The existence of two orientations in the asymmetric unit indicates that these interactions are not directional but perhaps largely dispersive and/or electrostatic.

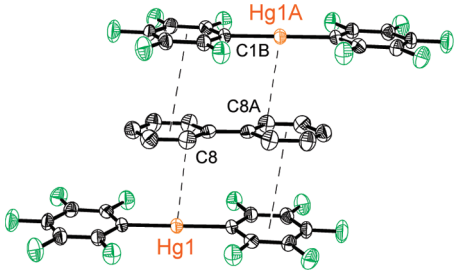

Figure 4. ORTEP view (30% ellipsoid) of a portion of a stack in the structure of [**1**·biphenyl]. The representative intermolecular distance Hg(1)−C(8) is 3.51 Å.

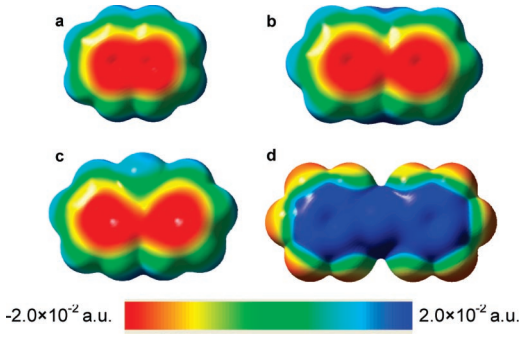

Figure 5. Electrostatic potential surfaces of (a) naphthalene, (b) biphenyl, (c) fluorene, and (d) **1**.

Solid-State Luminescence. All adducts give rise to a very intense photoluminescence in the visible region. At room temperature, the adducts [**1**·biphenyl] emit blue light whereas

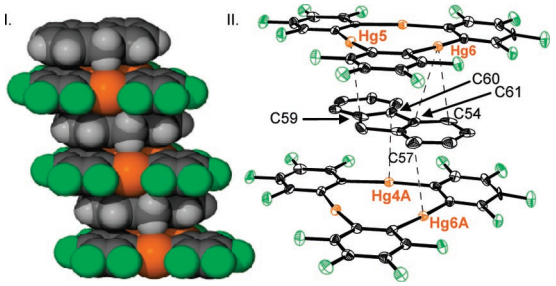

Figure 6. Space filling (left) and ORTEP view (50% ellipsoids, right) of a portion of a stack in the structure of [**2**·fluorene]. Only one of the two crystallographically independent stacks is shown. Representative intermolecular distances (Å): Hg(4A)−C(60) 3.29, Hg(5)−C(59) 3.29, Hg(6)−C(54) 3.27, Hg(6)−C(61) 3.39, Hg(6A)-C(57) 3.36.

[**1**·naphthalene], [**1**·fluorene], and [**2**·fluorene] give rise to a green emission (Figure 7). For a given adduct, finely powdered and single crystalline samples give rise to the same emission color. The energy and vibronic progression observed for the emission of crystalline solids [**1**·naphthalene] and [**1**·biphenyl] correspond almost exactly to that observed for the phosphorescence of free naphthalene or biphenyl in an EPA matrix at 77 K.[35] Similar observations have been made for arene adducts of the trinuclear complex **2**, which also display intense phosphorescence of the arene.[8] As previously proposed for [**2**·naphthalene] and [**2**·biphenyl],[8] the observed phosphorescence of [**1**·naphthalene] and [**1**·biphenyl] results from an external mercury heavy-atom effect which affects the photophysical properties of the arene. Taking into account the fact that the mercury atom of **1** is coordinated to the π-faces of the arene, such an external heavy-atom effect seems to constitute a valid explanation for the observed phosphorescence. In the case of the fluorene adducts, the emission spectrum shows a remarkable temperature dependence. At 4 K, the emission spectra of [**1**·fluorene] and [**2**·fluorene] show similar vibronic features to those reported for pure fluorene.[36] When the sample is warmed, the intensity of the high-energy vibronic peaks, especially the 0,0 transition, decreases and ultimately disappears above 15 K for [**1**·fluorene] and 45 K for [**2**·fluorene]. Changes in the vibronic peak distribution are not unusual for molecular systems; factors such as temperature, excitation wavelength, and sample phase or morphology can affect the relative intensities of vibronic transitions.[37]

The energy of the 0,0 transition in the emission spectrum of adducts involving the trinuclear **2** are distinctly red-shifted when compared to the corresponding adducts involving **1**, which are themselves red-shifted when compared to the triplet emission of the pure arene in *n*-heptane matrices (Table 2). These red shifts suggest that the T_1 state of the arene is stabilized by interaction with the organomercurial. Elaborating on this idea, we propose that the orbital of the organomercurial involved in this interaction is the LUMO. Unlike in **1** where the LUMO bears the contribution of a single mercury 6p orbital, the LUMO of **2** results from the mixing of three mercury 6p orbitals and is therefore expected to have a lower energy.[6] With a lower energy, the LUMO of **2** may interact more strongly with filled orbitals of the exited arene. In other words, the proximity of the three mercury centers serves to enhance the Lewis acidity of **2** which becomes a better acceptor. These conclusions are in agreement with a charge-transfer model[38,39] developed several decades ago to explain the occurrence of external heavy-atom effects. Inspection of the luminescence excitation spectra of the adducts leads to the same general conclusion (Figure 7). In all cases, the excitation spectra feature a broad band that is distinctly red-shifted when compared to the absorption of the arene and organomercurials,[40] suggesting a charge-transfer assignment for the excitation route similar to that proposed by Fackler and co-workers for a binary adduct involving a trinuclear Au(I) complex and octafluoronaphthalene.[41] While the above evidence is in agreement with the charge-transfer nature of the external heavy-atom effects, an exchange mechanism in which the organomercurial would act as a triplet energy donor cannot be entirely ruled out. Such mechanisms are well accounted for by the Robinson theory[42] and have been previously invoked to rationalize the photophysical properties of $MeHg^{II}$ adducts of various substrates including tryptophan.[43]

To better compare the extent of the heavy-atom effects induced by **1** and **2** in the solid state, we have measured the kinetics of the radiative decay for each adduct. The triplet-state lifetimes for [**1**·naphthalene], [**1**·biphenyl], [**1**·fluorene], and [**2**·fluorene] as well as those previously reported[7] are shown for comparison in Table 3. In all cases, the lifetimes are shorter than those of the free arenes (2.3, 4.4, and 6.3 *seconds* for naphthalene in EPA glass, biphenyl in EPA glass, and fluorene in ethanol glass, respectively),[35,36] which is indicative of the heavy-atom effect caused by the presence of mercury. However, the arene adducts of the trinuclear organomercurial **2** have triplet-state lifetimes that are significantly shorter than those of [**1**·naphthalene], [**1**·biphenyl], and [**1**·fluorene] (Table 3). The $(\tau^P)^{-1}$ values measured at 77 K or *RT* represent the sum of the radiative (k_r) and nonradiative (k_{nr}) decay rate constants, which cannot be readily separated. Hence, we have carried out low-temperature lifetime measurements down to 4 K (Table 3). Extrapolation of the low-temperature data down to 0 K provides estimation for the k_r values, which are presented in

(35) Gustav, K.; Seydenschwanz, C. *Chem. Phys. Lett.* **1984**, *109*, 156−159. (b) Ramamurthy, V.; Eaton, D. F.; and Caspar, J. V. *Acc. Chem. Res.* **1992**, *25*, 299−307.
(36) Najbar, J.; Barzyk, W. *J. Lumin.* **1974**, *8*, 242−251. (b) Bree, A.; Zwarich, R. *J. Chem. Phys.* **1969**, *51*, 903−912.
(37) For example, see: (a) Becker, R. S.; Dolan, E.; Balke, D. E. *J. Chem. Phys.* **1969**, *50*, 239−245.(b) Becker, R. S.; Pelliccioli, A. P.; Romani, A.; Favaro, G. *J. Am. Chem. Soc.* **1999**, *121*, 2104−2109. (c) Favaro, G.; Romani, A.; Becker, R. S. *Photochem. Photobiol.* 2001, *74*, 378−384. (d) Gentili, P. L.; Romani, A.; Becker, R. S.; Favaro, G. *Chem. Phys.* **2005**, *309*, 167−175.
(38) Melhiush, W. H.; Metcalf, W. S. *J. Chem. Soc.* **1958**, 480−482.
(39) McGlynn, S. P.; Azumi, T.; Kinoshita, M. *Molecular Spectroscopy of the Triplet State*; Prentice Hall: Englewood Cliffs, NJ, 1969; Chapter 8, pp 311−314.
(40) The absorption spectra of **1** and **2** overlaid with those of the arene and the excitation spectra of the adducts can be found in the Supporting Information.
(41) Mohamed, A. A.; Rawashdeh-Omary, M. A.; Omary, M. A.; Fackler, J. P., Jr. *Dalton Trans.* **2005**, 2597.
(42) Robinson, G. W. *J. Chem. Phys.* **1967**, *46*, 572.
(43) Svejda, P.; Maki, A. H.; Anderson, R. R. *J. Am. Chem. Soc.* **1978**, *100*, 7138−7145.

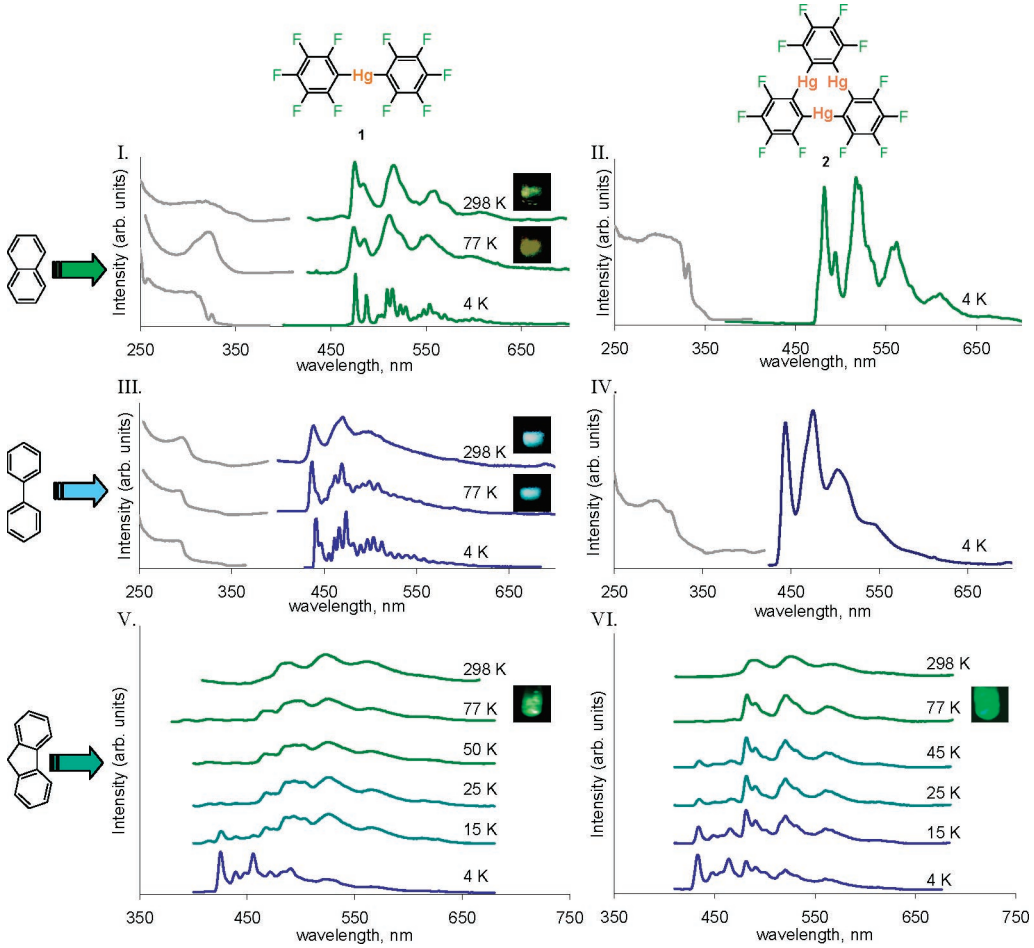

Figure 7. Excitation and emission of the solid adduct of [**1**·naphthalene] ($\lambda_{excited}$ = 320 nm) (I), [**2**·naphthalene] ($\lambda_{excited}$ = 300 nm) (II), [**1**·biphenyl] ($\lambda_{excited}$ = 290 nm) (III), [**2**·biphenyl] ($\lambda_{excited}$ = 295 nm) (IV), [**1**·fluorene] ($\lambda_{excited}$ = 300 nm) (V), and [**2**·fluorene] ($\lambda_{excited}$ = 320 nm) (VI) at the temperatures noted. The pictures in the insets show the emission color observed under a handheld UV lamp. The pictures shown for the fluorene adducts are taken immediately after immersion of the sample in liquid nitrogen. At room temperature, both fluorene adducts give rise to a green emission (not shown).

Table 2. Comparison of the 0,0 Energy Transitions in cm^{-1} between the Free Arene and the Adducts Involving **1** and **2** at 4 K

	free arene $\nu(0,0)$ (cm^{-1})	adduct with **1** $\nu(0,0)$ (cm^{-1})	$\Delta\nu^a$ (cm^{-1})	adduct with **2** $\nu(0,0)$ (cm^{-1})	$\Delta\nu^a$ (cm^{-1})
naphthalene	21 277[b]	21 008	269	20 747	803
biphenyl	23 041[c]	22 624	417	22 472	569
fluorene	23 810[d]	23 474	336	23 041	769

[a] $\Delta\nu = \nu(0,0)$ of the free arene$-\nu(0,0)$ of the adduct with the organomercurial. [b] Reference 45. [c] Reference 46. [d] Reference 36b.

Table 3. Radiative Rate Constants and Triplet Lifetimes for Naphthalene, Biphenyl, and Fluorene Adducts of **1** and **2**

	k_r/s^{-1}	τ_{4K}/ms	τ_{77K}/ms	τ_{RT} /ms
[**1**·naphthalene]	139	7.71	5.15	3.11
[**1**·biphenyl]	209	4.77	2.96	2.60
[**1**·fluorene]	264	3.32	1.56	0.976
[**2**·naphthalene]	669	1.42	0.985[a]	0.712[a]
[**2**·biphenyl]	1 091	0.891	0.337[a]	0.454[a]
[**2**·fluorene]	1 469	0.657	0.436	0.265

[a] Values taken from ref 7.

Table 3. In all cases, arene adducts of **2** have a higher k_r than the corresponding arene adducts of **1**. The ratios of k_r([**2**·arene])/k_r([**1**·arene]) are almost equal (4.8 for naphthalene, 5.5 for biphenyl, and 5.2 for fluorene). The drastic shortening in the lifetimes and increase in k_r values for arene adducts of **2** vs **1** demonstrate cooperative effects between the three mercury centers in **2** that lead to more efficient phosphorescence via external heavy-atom effects. These cooperative effects are even more drastic than those known for organic systems with internal heavy-atom effects. For example, the τ^P value changes from 17.6 to 4.96 ms on going from 2-bromonaphthalene to 1,2,4-tribromonaphthalene in EPA glass.[44]

Concluding Remarks

The results reported in these studies indicate that simple mononuclear organomercurials such as **1** readily assemble with arenes to form room-temperature phosphorescent supramolecules with short triplet lifetimes. Keeping in mind that **1** can be prepared in one step from simple starting materials, these results are important and may provide new routes to luminescent materials, a venue that we are currently investigating. The second important aspect of this work concerns the finding that **2**, unlike **1**, quenches the fluorescence of naphthalene in CH_2Cl_2. When compared to **1**, the high quenching efficiency of **2** may be correlated to the higher

(44) Pavlopoulos, T. G. *Mol. Phys.* **1968**, *14*, 87−92.
(45) Lim, E. C.; Li, Y. H. *J. Chem. Phys.* **1970**, *52*, 6416−6422.
(46) Miller, J. C.; Meek, J. S.; Strickler, S. J. *J. Am. Chem. Soc.* **1977**, *99*, 8175−8179.

affinity that **2** displays for arenes as well as to more acute external heavy-atom effects caused by the three mercury atoms. The photophysical results reported herein suggest that, at least in the exited state, the arene interacts with organomercurials. These interactions may be involved in the pathway allowing the arene to borrow spin−orbit coupling from the mercury atoms. Finally, both solution and solid-state studies show that the presence of three mercury atoms in **2** makes it a more efficient external heavy-atom-effect inducer.

Acknowledgment. M.I.B. was supported by an NSF-REU grant (CHE-0243829). This work is supported by the Texas Advanced Technology Program (Grant 010366-0039-2003 to F.P.G. and M.A.O.), the donors of the American Chemical Society Petroleum Research Fund (Grant 38143 -AC 3 to F.P.G.), the Welch Foundation (Grant B-1542 to M.A.O.), and NSF (CAREER Award CHE-0349313 to M.A.O.). We thank the anonymous referees for their help with this paper.

Supporting Information Available: Lifetime measurements for the fluorescence titration of naphthalene by **2**; UV−vis absorption spectra of **1** and **2** overlaid with those of the arene and the excitation spectra of the adducts; calculation of the collisional quenching frequency for the system **2**/naphthalene; optimized structure of **1**; X-ray crystallographic data for [**1**•naphthalene], [**1**•biphenyl], [**1**•fluorene], and [**2**•fluorene] in CIF format. This material is available free of charge via the Internet at http://pubs.acs.org.

IC061998N